Communication in Physical Sciences, 2026, 13(7):1116-1138

Electrochemical Performance and Corrosion Protection of Zinc–Carbon Quantum Dot (Zn–CQD) Nanocomposite Coatings on Mild Steel

Nyeneime William Akpanudo

Received: 27 March 2026/Accepted: 18 June 2026/Published: 24 June 2026
doi.org/10.4314/cps.v13i7.6

Abstract: *Corrosion of mild steel in chloride-containing environments remains a major challenge for industrial infrastructure, necessitating the development of advanced protective coatings with enhanced electrochemical stability and durability. This study investigated the electrochemical performance and corrosion protection behavior of electrodeposited zinc–carbon quantum dot (Zn–CQD) nanocomposite coatings on mild steel. Carbon quantum dots (CQDs) were incorporated into a zinc sulfate electrolyte at concentrations of 0.0, 0.5, 1.0, 1.5, and 2.0 g L^{-1}, and the resulting coatings were evaluated using open circuit potential (OCP), potentiodynamic polarization, electrochemical impedance spectroscopy (EIS), microhardness, atomic force microscopy (AFM), water contact angle measurements, and ASTM B117 salt spray testing. Electrochemical results revealed a progressive reduction in corrosion current density from 18.6 μA cm^{-2} for bare mild steel to 1.12 μA cm^{-2} for the Zn–CQD-1.5 coating, while the charge-transfer resistance increased from 438 Ω cm^2 to 5215 Ω cm^2. Similarly, polarization resistance increased from 420 Ω cm^2 to 4978 Ω cm^2, accompanied by a reduction in corrosion rate from 0.214 to 0.013 mm $year^{-1}$, representing approximately 94% corrosion protection efficiency. Surface characterization demonstrated that CQD incorporation refined the coating microstructure, reducing average surface roughness from 198 nm for bare steel to 38 nm, while increasing Vickers microhardness from 182 $HV_{0.1}$ to 291 $HV_{0.1}$. The water contact angle increased from 61° to 108°, indicating enhanced hydrophobicity, whereas the corroded area after 500 h salt spray exposure decreased from 88% for bare steel to only 2.5% for Zn–CQD-1.5. However, excessive CQD loading (2.0 g L^{-1}) produced slight nanoparticle agglomeration that marginally reduced corrosion resistance. Overall, the Zn–CQD-1.5 nanocomposite coating exhibited the optimum combination of electrochemical stability, mechanical performance, and long-term corrosion protection, demonstrating the considerable potential of carbon quantum dots as sustainable nanoscale reinforcements for high-performance zinc protective coatings on mild steel.*

Keywords*: Carbon quantum dots; Zinc nanocomposite coating; Electrodeposition; Mild steel; Corrosion protection; Electrochemical impedance spectroscopy; Potentiodynamic polarization; Nanocoatings.*

Nyeneime William Akpanudo
Department of Chemistry, Akwa Ibom State University, Ikot Akpaden, Ikot Abasi, Akwa Ibom State, Nigeria.
Email: nyewills15@gmail.com
https://orcid.org/0000-0001-8095-6667

1.0 Introduction

Corrosion of metallic materials remains one of the greatest challenges confronting modern engineering and industrial infrastructure

Also available @ https://doi.org/10.5281/zenodo.21327759

because it leads to progressive deterioration of metals through electrochemical interactions with the surrounding environment (Eddy & Ita, 2011; Eddy *et al*., 2011, 2022). Mild steel is among the most extensively used engineering materials owing to its low cost, excellent mechanical strength, ease of fabrication, and weldability (Eddy *et al*., 2008, 2010). Consequently, it is widely employed in construction, pipelines, storage tanks, marine structures, automobiles, power plants, and chemical processing equipment (Odoemelam & Eddy, 2008; Odoemelam *et al*., 2009). Despite these advantages, mild steel exhibits poor corrosion resistance in aggressive environments containing chloride ions, acidic media, and moisture, resulting in rapid material degradation, structural failure, increased maintenance costs, environmental pollution, and safety hazards (Pan et al., 2024). Globally, corrosion is estimated to cost approximately US$2.5 trillion annually, representing about 3.4% of the world's gross domestic product, thereby emphasizing the urgent need for efficient and sustainable corrosion protection technologies (Pan et al., 2024).

Among the available corrosion mitigation strategies, metallic coatings remain one of the most effective approaches because they provide both physical barrier protection and electrochemical sacrificial protection. Zinc is the most widely used sacrificial coating for steel due to its more negative electrode potential relative to iron, enabling preferential anodic dissolution that protects the underlying steel even when the coating is locally damaged. Electrodeposition is particularly attractive because it is cost-effective, produces coatings with controllable thickness and composition, operates at relatively low temperatures, and can be readily adapted for industrial-scale production (Lemmadi et al., 2026; Abioye et al., 2019). However, conventional electrodeposited zinc coatings often suffer from microcracks, porosity, coarse grain structures, and localized defects that facilitate electrolyte penetration and eventually reduce long-term corrosion resistance (Yanardağ et al., 2023; Wang et al., 2025).

Recent advances in nanotechnology have transformed corrosion science through the development of nanostructured coatings capable of simultaneously improving barrier properties, mechanical strength, surface functionality, and electrochemical stability. Nanomaterials possess exceptionally high surface area, unique electronic properties, and excellent interfacial interactions, enabling them to modify coating microstructure at the nanoscale (Akpanudo & Olabemiwo, 2024a-c). Comprehensive reviews have demonstrated that nanomaterials can enhance coating compactness, reduce coating porosity, improve passivation behaviour, increase hydrophobicity, and provide multifunctional protection mechanisms including self-healing and controlled ion transport (Anadebe et al., 2026). Consequently, nanotechnology has emerged as a promising strategy for the development of next-generation corrosion-resistant coatings for marine, oil and gas, aerospace, and infrastructure applications.

Among carbon-based nanomaterials, carbon quantum dots (CQDs) have recently attracted considerable attention because of their extremely small particle size (<10 nm), high specific surface area, abundant oxygen- and nitrogen-containing functional groups, excellent water dispersibility, chemical stability, environmental friendliness, low toxicity, and ease of synthesis from renewable biomass and industrial waste resources (Eddy *et* al., 2024; Liu et al., 2026). Unlike graphene and carbon nanotubes, which frequently suffer from aggregation and poor dispersion within coating matrices, carbon quantum dots exhibit superior colloidal stability and strong interfacial interactions with metallic and polymeric systems. Their abundant functional groups promote improved adhesion between coating constituents while simultaneously refining coating microstructure through

enhanced nucleation during deposition (Dhongde et al., 2024; Liu et al., 2026). These characteristics enable CQDs to improve coating compactness, reduce ionic diffusion pathways, and significantly suppress electrochemical corrosion reactions.

Several recent investigations have demonstrated the effectiveness of carbon quantum dots in enhancing corrosion resistance. Dhongde et al. (2024) synthesized CQDs from rice husk biomass and incorporated them into epoxy coatings for carbon steel. Electrochemical impedance spectroscopy, potentiodynamic polarization, and salt spray testing showed that CQDs significantly enhanced corrosion resistance by improving coating adhesion and strengthening the epoxy–substrate interface through molecular interactions predicted by density functional theory. Similarly, Wang et al. (2022) reported that nitrogen-doped CQDs modified graphene-based waterborne epoxy coatings exhibited impedance values nearly 200 times higher than conventional epoxy coatings after prolonged immersion in 3.5 wt.% NaCl solution. The remarkable improvement was attributed to improved graphene orientation, enhanced interfacial bonding, and formation of stable protective films that inhibited electrolyte transport.

Recent work has also demonstrated the effectiveness of carbon quantum dots in metallic composite coatings. Duarte et al. (2024) produced electrodeposited tin–carbon quantum dot composite coatings and reported that an optimum CQD concentration produced a finer, more homogeneous coating microstructure with significantly improved corrosion resistance compared with pure tin coatings. Surface characterization by SEM, AFM, XRD, and XPS confirmed that CQDs promoted uniform crystal growth while reducing oxidation of the metallic coating. Likewise, Mohamed et al. (2026) fabricated biomass-derived CQD-containing superhydrophobic coatings on steel through a one-step electrodeposition process. The incorporation of CQDs fundamentally altered coating nucleation, producing dense granular structures with a water contact angle of 167°, improved abrasion resistance, and corrosion protection efficiency exceeding 93%, demonstrating the multifunctional benefits of CQD incorporation.

Apart from carbon quantum dots, numerous studies have shown that nanoparticle incorporation markedly improves the electrochemical performance of zinc-based coatings. Barsana et al. (2025) incorporated CeO_2 and CeO_2–CuO nanoparticles into zinc phosphate coatings and observed substantial reductions in corrosion current density together with significant increases in polarization resistance and charge-transfer resistance owing to the formation of compact coating structures. Similarly, Jayaramaiah and Yanjerappa (2026) demonstrated that Zn–$Cu_2V_2O_7$ composite coatings exhibited higher charge-transfer resistance, lower corrosion current density, and enhanced hydrophobicity compared with pure zinc coatings because the nanoparticles refined the zinc microstructure and minimized coating porosity. Ayub et al. (2025) further reported that graphene-reinforced zinc coatings produced protection efficiencies exceeding 60% improvement over graphene-free coatings due to enhanced barrier properties and reduced diffusion of corrosive species. ZnO-based hybrid coatings have also been shown to significantly improve corrosion resistance through synergistic interactions between zinc oxide nanoparticles, epoxy, and polymer matrices (Suhas & Shanmugapriya, 2025). These investigations collectively demonstrate that nanoparticle reinforcement is an effective strategy for improving the electrochemical performance of zinc coatings.

Carbon-based nanomaterials have also been extensively investigated as environmentally friendly corrosion inhibitors in both acidic and neutral environments. Reviews by Pan et al. (2024) and Liu et al. (2026) conclude that

carbon nanomaterials improve corrosion protection by increasing coating tortuosity, reducing ionic transport, promoting passive film formation, and strengthening coating adhesion. Earlier studies by Eddy and co-workers established the effectiveness of environmentally benign corrosion inhibitors derived from plant extracts, pharmaceuticals, and organic molecules for protecting mild steel and zinc through adsorption mechanisms, quantum chemical interactions, and synergistic effects (Eddy, 2010; Eddy & Ita, 2011; Eddy et al., 2011; Eddy et al., 2022; Eddy et al., 2010). These investigations have contributed significantly to the understanding of corrosion inhibition mechanisms and demonstrate the growing transition toward sustainable corrosion protection technologies.

Despite the remarkable progress achieved in nanostructured corrosion-resistant coatings, significant knowledge gaps remain. Most published studies involving carbon quantum dots have concentrated on polymeric coatings such as epoxy systems (Dhongde et al., 2024; Wang et al., 2022), superhydrophobic coatings (Mohamed et al., 2026), or metallic systems based on tin (Duarte et al., 2024). Comparatively few studies have investigated the direct incorporation of carbon quantum dots into electrodeposited zinc coatings for mild steel substrates. Furthermore, the influence of CQD concentration on the electrochemical behaviour, polarization resistance, corrosion rate, microhardness, surface morphology, wettability, and long-term salt spray performance of zinc nanocomposite coatings has not been comprehensively established. The microstructural mechanisms through which CQDs modify zinc crystal growth and optimize corrosion protection also remain insufficiently understood. Addressing these limitations is essential for developing advanced zinc-based nanocomposite coatings suitable for severe industrial and marine environments.

Therefore, this study aimed to investigate the electrochemical performance and corrosion protection behaviour of electrodeposited zinc–carbon quantum dot (Zn–CQD) nanocomposite coatings on mild steel. Carbon quantum dots were incorporated into the zinc electrodeposition bath at different concentrations to determine the optimum nanoparticle loading for maximum corrosion protection. The coatings were evaluated using open circuit potential (OCP), potentiodynamic polarization, electrochemical impedance spectroscopy (EIS), polarization resistance measurements, corrosion rate determination, microhardness testing, atomic force microscopy (AFM), water contact angle measurements, and accelerated ASTM B117 salt spray testing. The relationships between CQD concentration, coating microstructure, electrochemical behaviour, and corrosion resistance were systematically examined.

The significance of this study lies in the development of an advanced zinc-based nanocomposite coating that integrates the sacrificial protection of zinc with the unique nanoscale reinforcement provided by carbon quantum dots. The findings provide new insights into the role of CQDs in refining zinc electrodeposition, improving coating compactness, enhancing mechanical properties, increasing hydrophobicity, and suppressing electrochemical corrosion processes. In addition, the study contributes to the growing field of sustainable nanotechnology by demonstrating the potential application of environmentally benign carbon quantum dots—including those synthesized from biomass and abundant low-grade coal resources (Eddy et al., 2026)—for next-generation corrosion-resistant coatings. The developed Zn–CQD nanocomposite coatings have significant potential for protecting mild steel components used in marine structures, pipelines, bridges, automobiles, chemical plants, and other industrial systems exposed to aggressive chloride-containing environments.

2.0 Materials and Methods

2.1 Materials

Commercial low-carbon mild steel sheets were used as the substrate material for electrodeposition. The mild steel possessed a nominal composition (wt.%) of C (0.18), Mn (0.45), Si (0.22), P (0.03), S (0.03), with the balance being Fe. The steel was machined into coupons measuring 30 mm × 20 mm × 2 mm, providing an exposed working area of approximately 2.0 cm^2 during electrochemical measurements.

Analytical-grade zinc sulfate heptahydrate ($ZnSO_4·7H_2O$), sodium sulfate (Na_2SO_4), boric acid (H_3BO_3), potassium chloride (KCl), sodium hydroxide (NaOH), hydrochloric acid (HCl), acetone, ethanol, silicon carbide abrasive papers (400–2000 grit), and distilled water were used throughout the study. Carbon quantum dots (CQDs) synthesized from lignite coal using the oxidation method described by Eddy et al. (2026) were employed as reinforcing nanoparticles. The CQDs possessed an average particle size below 10 nm with abundant oxygen-containing functional groups that promoted good dispersion within the electrolyte.

The electrodeposition bath was prepared using distilled water, while all electrochemical measurements were carried out in naturally aerated 3.5 wt.% NaCl solution, prepared according to ASTM G5/G59 recommendations to simulate marine exposure conditions.

2.2 Preparation of Mild Steel Specimens

Prior to coating, the mild steel coupons were mechanically polished sequentially using silicon carbide abrasive papers of 400, 600, 800, 1200, 1500, and 2000 grit to obtain a smooth metallic surface. The polished specimens were thoroughly rinsed with distilled water, ultrasonically cleaned in ethanol for 10 min, degreased with acetone, and finally dried under warm air.

Surface activation was performed by immersing the cleaned specimens in 10 wt.% HCl solution for 30 s, followed by immediate rinsing with distilled water to remove residual oxides. The activated samples were then dried and stored in a desiccator before electrodeposition.

2.3 Preparation of Zinc–Carbon Quantum Dot Electrolyte

The zinc electrodeposition bath consisted of 150 g L^{-1} $ZnSO_4·7H_2O$, 30 g L^{-1} Na_2SO_4, and 25 g L^{-1} H_3BO_3. Boric acid acted as a buffering agent to stabilize bath pH and improve coating quality.

Carbon quantum dots were dispersed into separate electrolyte baths at concentrations of 0.0, 0.5, 1.0, 1.5, and 2.0 g L^{-1}. Each suspension was ultrasonically agitated for 60 min before electrodeposition to ensure homogeneous nanoparticle dispersion and minimize agglomeration.

2.4 Electrodeposition of Zn–CQD Nanocomposite Coatings

Electrodeposition was carried out using a conventional three-electrode electrochemical cell connected to a programmable DC power supply. The prepared mild steel coupon served as the cathode, while a high-purity zinc plate (99.99%) was employed as the sacrificial anode.

The deposition conditions were maintained as follows:

Parameter	Value
Current density	2.5 A dm^{-2}
Deposition time	20 min
Bath temperature	30 ± 2 °C
Bath pH	4.5
Stirring speed	250 rpm

Five coating systems were produced including Zn (without CQDs) , Zn–CQD-0.5, Zn–CQD-1.0, Zn–CQD-1.5 and Zn–CQD-2.0 /

Following electrodeposition, the coated specimens were rinsed thoroughly with distilled water, washed with ethanol, air-dried, and stored in a desiccator for 24 h before characterization.

2.5 Electrochemical Characterization

Electrochemical evaluation was performed using a computer-controlled potentiostat/galvanostat equipped with impedance measurement capability. A conventional three-electrode electrochemical cell was employed consisting of the coated mild steel as the working electrode, a platinum mesh as the counter electrode, and an Ag/AgCl electrode as the reference electrode.

2.5.1 Open Circuit Potential (OCP)

Open circuit potential measurements were conducted immediately after immersion of each specimen in 3.5 wt.% NaCl solution. The potential evolution was monitored continuously for 3600 s until a stable equilibrium potential was attained.

3.5.2 Potentiodynamic Polarization (Tafel Analysis)

Potentiodynamic polarization measurements were performed after OCP stabilization by scanning from −250 mV to +250 mV relative to the open circuit potential at a scan rate of 1 mV s^{-1}.

The corrosion current density (Icorr) and corrosion potential (Ecorr) were determined by Tafel extrapolation according to ASTM G59.

2.5.3 Electrochemical Impedance Spectroscopy (EIS)

Electrochemical impedance spectroscopy measurements were carried out at the stabilized OCP using an AC perturbation amplitude of 10 mV over a frequency range of
100 kHz to 0.01 Hz. Nyquist and Bode plots were analyzed using an equivalent electrical circuit to determine the electrochemical parameters governing coating performance.

2.6 Determination of Corrosion Parameters

The electrochemical parameters extracted from polarization and impedance analyses included corrosion potential (Ecorr), corrosion current density (Icorr), anodic Tafel slope (βa), cathodic Tafel slope (βc), solution resistance (Rs), charge-transfer resistance (Rct), double-layer capacitance (Cdl), polarization resistance (Rp), corrosion rate, and coating protection efficiency.

The corrosion rate (CR) was calculated using equation 1, which is an ASTM G102 approach

$$CR = \frac{0.00327 \times I_{corr} \times EW}{\rho} \quad (1)$$

where: CR = corrosion rate (mm $year^{-1}$), i_{corr} = corrosion current density (μA cm^{-2}), EW = equivalent weight of mild steel, and ρ = density of mild steel (g cm^{-3}).

The coating protection efficiency (PE) was determined using equation 2

$$PE(\%) = \frac{I^0_{corr} - I_{corr}}{I^0_{corr}} \times \frac{100}{1} \quad (2)$$

where $PE(\%)$ defines the coating protection efficiency I_{corr} is to the corrosion current density of the uncoated mild steel, and I^0_{corr} represents the corrosion current density of the zinc-coated specimen

Polarization resistance (Rp) was estimated using the Stern–Geary relationship, expressed as equation 3

$$R_p = \frac{\beta_a \beta_c}{2.303 I_{corr}(\beta_a + \beta_c)} \quad (3)$$

where β_a and β_c represent the anodic and cathodic Tafel slopes, respectively.

3.7 Salt Spray Test

Accelerated corrosion testing was conducted according to ASTM B117 using a neutral salt spray chamber containing 5 wt.% NaCl solution maintained at 35 ± 2 °C. The coated specimens were exposed continuously for 500 h, after which the percentage corroded area was determined using digital image analysis.

3.0 Results and Discussion

3.1 Open Circuit Potential (OCP)

Open Circuit Potential (OCP) measurements provide valuable information on the thermodynamic tendency of a metal to undergo corrosion upon exposure to an electrolyte. The evolution of the OCP with immersion time reflects the electrochemical stability of the coating and the establishment of equilibrium at the coating/electrolyte interface. In the present study, OCP measurements were conducted for bare mild steel and Zn–CQD nanocomposite-

coated specimens during immersion in 3.5 wt.% NaCl solution. The OCP evolution curves are presented in Fig. 1(a), while the stabilized OCP values are summarized in Table 1.

As illustrated in Fig. 1(a), all specimens exhibited a gradual decrease in OCP during the initial stages of immersion, followed by stabilization after approximately 1500–1800 s. The initial negative shift is attributed to the activation of the metallic surface immediately after immersion and the establishment of electrochemical equilibrium between the electrode and the chloride electrolyte. After stabilization, only minor fluctuations in potential were observed, indicating that a relatively stable surface condition had been attained for both the bare and coated specimens.

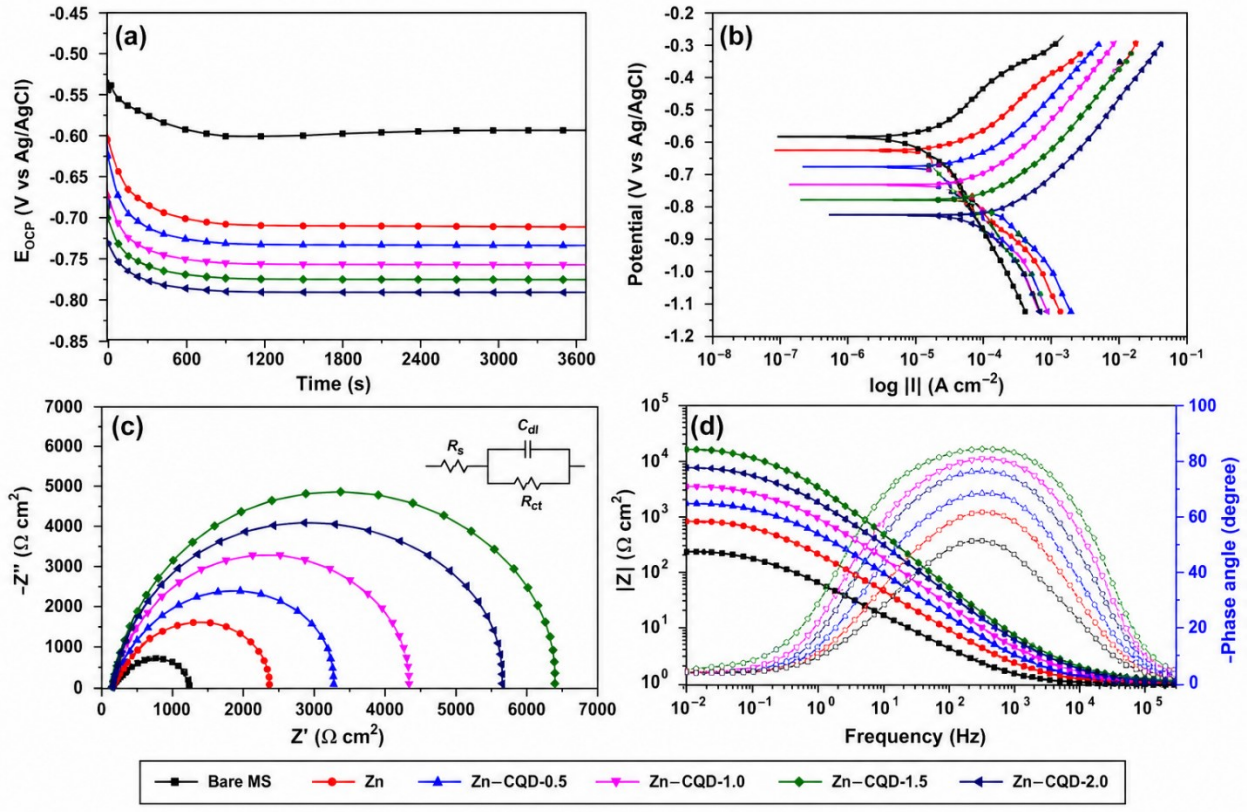

Fig. 1. Electrochemical characterization of bare mild steel and Zn–CQD nanocomposite coatings in 3.5 wt.% NaCl solution. (a) Open circuit potential (OCP) evolution during immersion, showing stabilization of the corrosion potential with increasing coating quality. (b) Potentiodynamic polarization (Tafel) curves illustrating the reduction in corrosion current density and shift in corrosion potential after Zn–CQD deposition. (c) Nyquist impedance plots demonstrating the increase in charge-transfer resistance with CQD incorporation. (d) Bode impedance plots showing the impedance modulus and phase angle as a function of frequency, indicating enhanced barrier properties and electrochemical stability of the Zn–CQD coatings.

The uncoated mild steel exhibited the highest (least negative) stabilized potential of −0.612 V, indicating its greater thermodynamic susceptibility to active corrosion in chloride solution (Table 1). Following zinc electrodeposition, the OCP shifted markedly towards more negative values, decreasing to −0.748 V for the pure zinc coating. Progressive incorporation of carbon quantum dots (CQDs) into the zinc matrix produced further negative

shifts in potential, reaching −0.764 V, −0.781 V, and −0.792 V for Zn–CQD-0.5, Zn–CQD-1.0, and Zn–CQD-1.5 coatings, respectively. The Zn–CQD-2.0 coating exhibited a slightly less negative stabilized potential (−0.785 V) than Zn–CQD-1.5, suggesting that excessive CQD incorporation did not further improve the electrochemical activity of the coating.

The observed negative shift in OCP with increasing CQD content indicates enhanced sacrificial protection of the mild steel substrate. Since zinc possesses a lower electrode potential than iron, it preferentially undergoes anodic dissolution, thereby protecting the underlying steel through galvanic action. The incorporation of CQDs appears to improve this sacrificial behaviour by promoting the formation of a more compact and electrochemically active coating. Carbon quantum dots act as nanoscale reinforcement particles that refine the electrodeposited zinc grains, reduce coating porosity, and improve coating uniformity. Consequently, electrolyte penetration to the steel surface is minimized, while the zinc coating remains electrochemically active enough to provide efficient cathodic protection.

Table 1. Stabilized Open Circuit Potential

Sample	CQD ($g\ L^{-1}$)	Stable OCP (V vs Ag/AgCl)
Bare MS	0.0	-0.612
Zn	0.0	-0.748
Zn-CQD-0.5	0.5	-0.764
Zn-CQD-1.0	1.0	-0.781
Zn-CQD-1.5	1.5	-0.792
Zn-CQD-2.0	2.0	-0.785

The slight positive shift observed for the Zn–CQD-2.0 coating relative to Zn–CQD-1.5 suggests that excessive nanoparticle loading may adversely influence coating quality. At higher concentrations, CQDs tend to agglomerate within the electrolyte, leading to localized defects and non-uniform particle distribution during electrodeposition. These agglomerates can interfere with zinc nucleation and crystal growth, producing microscopic discontinuities that reduce coating compactness and slightly diminish the effectiveness of sacrificial protection. Similar behaviour has been widely reported for nanoparticle-reinforced electrodeposited coatings, where an optimum nanoparticle concentration exists beyond which coating performance begins to deteriorate.

The OCP results are in excellent agreement with the subsequent electrochemical measurements presented in Fig. 1(b–d). The coating exhibiting the most negative stabilized potential (Zn–CQD-1.5) also displayed the lowest corrosion current density, the largest Nyquist semicircle, and the highest impedance modulus, indicating superior corrosion resistance. Likewise, the Zn–CQD-2.0 coating showed a slight reduction in electrochemical performance, confirming that the optimum CQD incorporation had been exceeded. This strong correlation demonstrates that OCP measurements provide an effective preliminary indicator of coating performance before detailed electrochemical characterization.

The present findings are consistent with previous studies on zinc-based nanocomposite coatings. Jayaramaiah and Yanjerappa (2026) reported that Zn–$Cu_2V_2O_7$ composite coatings exhibited more negative corrosion potentials than pure zinc coatings because nanoparticle incorporation improved coating compactness and electrochemical stability. Similarly, Ayub et al. (2025) demonstrated that graphene-reinforced zinc coatings exhibited enhanced corrosion resistance due to improved barrier properties and reduced electrolyte diffusion. Comparable improvements in electrochemical stability have also been reported for ZnO-based hybrid coatings and graphene-modified zinc coatings, where nanoparticles promoted finer microstructures and reduced coating defects, leading to improved sacrificial protection and lower corrosion activity.

Overall, the OCP results demonstrate that the incorporation of carbon quantum dots substantially enhanced the electrochemical behaviour of electrodeposited zinc coatings. The Zn–CQD-1.5 coating exhibited the most favourable electrochemical response, achieving the most negative stabilized OCP (−0.792 V vs Ag/AgCl), which is indicative of the highest sacrificial protection capability. The slight decline observed for Zn–CQD-2.0 further confirms that 1.5 g L^{-1} CQD represents the optimum nanoparticle concentration for producing dense, uniform, and highly protective Zn–CQD nanocomposite coatings on mild steel.

3.2 Potentiodynamic Polarization

Potentiodynamic polarization is one of the most reliable electrochemical techniques for evaluating the corrosion behaviour of metallic materials and protective coatings. The method provides quantitative information on the corrosion potential (Ecorr), corrosion current density (Icorr), anodic Tafel slope (βa), and cathodic Tafel slope (βc), which collectively describe the kinetics of the anodic metal dissolution and cathodic reduction reactions. Lower corrosion current density and more negative corrosion potential generally indicate improved sacrificial protection and enhanced corrosion resistance of zinc-coated systems. The potentiodynamic polarization curves of the bare and Zn–CQD-coated specimens are presented in Fig. 1(b), while the electrochemical parameters obtained from Tafel extrapolation are summarized in Table 2.

Table 2. Electrochemical parameters obtained from potentiodynamic polarization (Tafel) analysis of bare mild steel and Zn–CQD nanocomposite coatings in 3.5 wt.% NaCl solution.

Sample	E_{corr} (V)	I_{corr} (μA cm^{-2})	β_a (mV dec^{-1})	β_c (mV dec^{-1})
Bare MS	-0.612	18.6	118	136
Zn	-0.748	4.92	95	108
Zn–CQD-0.5	-0.764	3.28	91	102
Zn–CQD-1.0	-0.781	1.86	84	96
Zn–CQD-1.5	-0.792	1.12	80	91
Zn–CQD-2.0	-0.785	1.48	82	95

The potentiodynamic polarization curves shown in Fig. 1(b) reveal a significant improvement in the corrosion behaviour of mild steel following zinc electrodeposition and subsequent incorporation of carbon quantum dots. The coated specimens exhibited a systematic shift of the polarization curves toward lower current densities compared with the bare substrate, indicating substantial suppression of the electrochemical corrosion reactions. In addition, the corrosion potentials shifted progressively toward more negative values, confirming that the zinc-based coatings provided sacrificial anodic protection to the underlying steel.

The electrochemical parameters presented in Table 2 demonstrate a remarkable reduction in corrosion current density with increasing CQD incorporation. The bare mild steel exhibited the highest corrosion current density of 18.6 μA cm^{-2}, reflecting rapid electrochemical dissolution in the chloride medium. Following zinc deposition, the corrosion current decreased to 4.92 μA cm^{-2}, representing a reduction of approximately 74% relative to the uncoated specimen. Further incorporation of CQDs continuously reduced the corrosion current to 3.28, 1.86, and 1.12 μA cm^{-2} for Zn–CQD-0.5, Zn–CQD-1.0, and Zn–CQD-1.5, respectively. This progressive decline indicates

that the Zn–CQD nanocomposite coatings increasingly inhibited electrochemical charge transfer and restricted corrosion reactions at the coating/electrolyte interface. The Zn–CQD-1.5 coating exhibited the lowest corrosion current density, corresponding to an overall reduction of approximately 94% compared with bare mild steel.

A slight increase in corrosion current density to 1.48 μA cm^{-2} was observed for the Zn–CQD-2.0 coating (Table 2). Although this coating still provided excellent corrosion resistance, the increase suggests that excessive CQD incorporation may have reduced coating quality. At higher nanoparticle concentrations, CQDs tend to agglomerate within the electrodeposition bath, producing localized particle clusters that interfere with uniform zinc crystal growth. These agglomerates may introduce microscopic defects and increase coating porosity, thereby creating preferential pathways for electrolyte penetration and slightly increasing the corrosion rate. This behaviour indicates that 1.5 g L^{-1} represents the optimum CQD concentration for achieving maximum corrosion protection under the present deposition conditions.

The corrosion potential values followed a similar trend to the OCP results discussed previously. The corrosion potential shifted from −0.612 V for bare mild steel to −0.748 V for the pure zinc coating and reached −0.792 V for Zn–CQD-1.5 (Table 2). The increasingly negative corrosion potentials demonstrate that the Zn–CQD coatings remained electrochemically more active than the steel substrate and therefore preferentially underwent anodic dissolution. This behaviour is characteristic of effective galvanic protection, whereby zinc corrodes sacrificially while preserving the integrity of the underlying mild steel. The slightly less negative corrosion potential observed for Zn–CQD-2.0 (−0.785 V) further supports the conclusion that excessive CQD loading slightly diminished the sacrificial efficiency of the coating.

The anodic (βa) and cathodic (βc) Tafel slopes also decreased progressively with increasing CQD content, from 118 and 136 mV dec^{-1} for bare mild steel to 80 and 91 mV dec^{-1}, respectively, for Zn–CQD-1.5 (Table 2). The reduction in βa indicates that the anodic dissolution of zinc and iron became increasingly inhibited due to the formation of a dense nanocomposite coating, while the lower βc values suggest that the cathodic oxygen reduction reaction was similarly suppressed. These observations indicate that the Zn–CQD coatings function as mixed-type protective coatings by simultaneously reducing both anodic and cathodic electrochemical reactions. The presence of uniformly dispersed CQDs likely enhanced coating compactness, reduced microstructural defects, and increased the tortuosity for chloride ion diffusion, thereby decreasing the kinetics of both corrosion processes.

The polarization results correlate strongly with the other electrochemical measurements presented in Fig. 1(a), Fig. 1(c), and Fig. 1(d). The Zn–CQD-1.5 coating, which exhibited the lowest corrosion current density, also showed the most negative stabilized open-circuit potential, the largest Nyquist capacitive loop, and the highest impedance modulus across the investigated frequency range. These complementary observations confirm that the reduction in corrosion current was accompanied by increased charge-transfer resistance and superior barrier properties. Conversely, the slight deterioration in performance observed for Zn–CQD-2.0 is consistently reflected in all electrochemical techniques, demonstrating the reliability of the experimental data.

The present findings agree well with previous investigations on zinc-based nanocomposite coatings. Ayub et al. (2025) reported that graphene-reinforced zinc coatings exhibited significantly lower corrosion current densities due to improved coating compactness and reduced electrolyte permeability. Similarly,

Jayaramaiah and Yanjerappa (2026) demonstrated that Zn–$Cu_2V_2O_7$ nanocomposite coatings substantially reduced corrosion current while increasing charge-transfer resistance because uniformly dispersed ceramic nanoparticles refined the zinc microstructure. Comparable reductions in corrosion current have also been reported for ZnO-based hybrid coatings (Suhas & Shanmugapriya, 2025) and graphene-modified zinc coatings, where nanoparticle reinforcement enhanced barrier performance and delayed electrochemical degradation.

Overall, the potentiodynamic polarization results clearly demonstrate that the incorporation of carbon quantum dots significantly enhanced the corrosion resistance of electrodeposited zinc coatings. Among the investigated compositions, the Zn–CQD-1.5 coating exhibited the optimum electrochemical performance, achieving the lowest corrosion current density (1.12 μA cm^{-2}), the most negative corrosion potential (−0.792 V), and the greatest suppression of both anodic and cathodic reactions. These results confirm that the incorporation of an optimum concentration of carbon quantum dots substantially improves the protective performance of zinc coatings through enhanced coating compactness, reduced electrochemical activity, and improved resistance to chloride-induced corrosion.

3.3 Electrochemical Impedance Spectroscopy (EIS)

Electrochemical Impedance Spectroscopy (EIS) is a highly sensitive and non-destructive electrochemical technique widely used to evaluate the corrosion resistance and barrier properties of protective coatings. The technique provides insight into the electrochemical processes occurring at the coating/electrolyte interface by measuring the impedance response over a broad frequency range. In corrosion studies, the solution resistance (Rs), charge-transfer resistance (Rct), and double-layer capacitance (Cdl) are the principal electrochemical parameters used to assess coating performance. A higher charge-transfer resistance and lower double-layer capacitance generally indicate superior corrosion protection because they reflect restricted electron transfer and reduced electrolyte penetration through the coating. The Nyquist and Bode impedance plots obtained for the bare mild steel and Zn–CQD nanocomposite coatings are presented in Fig. 1(c) and Fig. 1(d), respectively, while the electrochemical parameters derived from equivalent circuit fitting are summarized in Table 3.

Table 3. Electrochemical impedance spectroscopy (EIS) parameters of bare mild steel and Zn–CQD nanocomposite coatings in 3.5 wt.% NaCl solution

Sample	Rs (Ω cm^2)	Rct (Ω cm^2)	Cdl (μF cm^{-2})
Bare MS	5.8	438	118
Zn	5.9	1698	61
Zn–CQD-0.5	5.9	2475	44
Zn–CQD-1.0	6.0	3828	29
Zn–CQD-1.5	6.1	5215	18
Zn–CQD-2.0	6.0	4687	22

The Nyquist impedance spectra shown in Fig. 1(c) exhibit a single depressed capacitive semicircle for all specimens, indicating that the corrosion process was predominantly controlled by charge-transfer reactions at the coating/electrolyte interface. The diameter of the capacitive semicircle increased markedly after zinc electrodeposition and became

progressively larger with increasing carbon quantum dot incorporation. Since the diameter of the Nyquist semicircle is directly proportional to the charge-transfer resistance, the results clearly demonstrate that the Zn–CQD coatings significantly improved the corrosion resistance of mild steel by inhibiting electrochemical charge transfer.

The quantitative EIS parameters presented in Table 3 confirm this behaviour. The bare mild steel exhibited the lowest charge-transfer resistance (438 Ω cm²), indicating rapid corrosion kinetics and unrestricted electron transfer between the steel surface and the chloride electrolyte. Following zinc deposition, the charge-transfer resistance increased nearly fourfold to 1698 Ω cm², confirming that the zinc coating effectively hindered corrosion reactions. Incorporation of carbon quantum dots produced a further increase in Rct to 2475 Ω cm², 3828 Ω cm², and 5215 Ω cm² for Zn–CQD-0.5, Zn–CQD-1.0, and Zn–CQD-1.5, respectively. These results indicate that the CQDs significantly enhanced the barrier properties of the zinc coating by producing a denser and more homogeneous microstructure that reduced electrolyte penetration and suppressed electron transfer across the coating interface.

The Zn–CQD-1.5 coating exhibited the highest charge-transfer resistance (5215 Ω cm²), representing approximately a 12-fold increase compared with bare mild steel. This substantial improvement confirms that the incorporation of an optimum concentration of carbon quantum dots markedly enhanced coating integrity and corrosion resistance. The enhanced performance can be attributed to the ability of CQDs to act as nanoscale grain refiners during electrodeposition. The nanoparticles promote uniform nucleation of zinc crystals, resulting in finer grains, lower porosity, improved coating compactness, and stronger adhesion to the steel substrate. These microstructural improvements increase the diffusion path for chloride ions and water molecules, thereby reducing corrosion activity. A slight decrease in charge-transfer resistance to 4687 Ω cm² was observed for the Zn–CQD-2.0 coating (Table 3). Although this value remained considerably higher than that of the pure zinc coating, the reduction suggests that excessive nanoparticle loading adversely affected coating quality. At higher concentrations, CQDs tend to agglomerate within the electrodeposition bath, producing localized particle clusters that interfere with uniform zinc deposition. The resulting microstructural defects and increased coating heterogeneity facilitate localized electrolyte penetration, thereby reducing charge-transfer resistance. This observation is consistent with the trends obtained from the OCP and polarization measurements, which also identified 1.5 g L^{-1} as the optimum CQD concentration.

The double-layer capacitance exhibited an opposite trend to the charge-transfer resistance. As shown in Table 3, Cdl decreased continuously from 118 μF cm^{-2} for bare mild steel to 61 μF cm^{-2} after zinc deposition and further declined to 44, 29, and 18 μF cm^{-2} for Zn–CQD-0.5, Zn–CQD-1.0, and Zn–CQD-1.5, respectively. The reduction in double-layer capacitance indicates a progressive decrease in the effective electrochemically active surface area exposed to the electrolyte. This behaviour results from improved coating compactness and reduced electrolyte adsorption at the coating surface. The lower capacitance values therefore confirm that CQD incorporation effectively minimized coating defects and increased resistance to electrolyte infiltration. A slight increase to 22 μF cm^{-2} for Zn–CQD-2.0 further supports the conclusion that excessive CQD incorporation introduced minor structural imperfections into the coating.

The Bode impedance plots presented in Fig. 1(d) provide additional evidence of improved coating performance. The Zn–CQD coatings exhibited substantially higher impedance

modulus values throughout the investigated frequency range than bare mild steel, indicating superior barrier properties and greater resistance to ionic transport. Furthermore, the Zn–CQD-1.5 coating displayed the highest phase angle and the broadest capacitive region, characteristic of a highly protective coating with excellent dielectric behaviour. The broad phase-angle maximum indicates that the coating remained electrically insulating over a wide frequency range, thereby limiting electrochemical reactions at the metal surface. The slight reduction in impedance observed for Zn–CQD-2.0 is again consistent with the minor decrease in Rct measured from the Nyquist analysis.

The EIS results correlate strongly with the potentiodynamic polarization and OCP measurements discussed in the preceding sections. The Zn–CQD-1.5 coating, which exhibited the highest charge-transfer resistance and lowest double-layer capacitance, also showed the lowest corrosion current density (1.12 μA cm^{-2}), the most negative corrosion potential (−0.792 V), and the highest protection efficiency. This strong agreement among the different electrochemical techniques confirms that improved corrosion resistance resulted from enhanced coating compactness and reduced electrochemical activity rather than measurement variability.

The present findings agree closely with previous reports on zinc-based nanocomposite coatings. Jayaramaiah and Yanjerappa (2026) reported that Zn–$Cu_2V_2O_7$ composite coatings significantly increased charge-transfer resistance because uniformly dispersed nanoparticles produced dense and hydrophobic coatings that restricted electrolyte penetration. Similarly, Ayub et al. (2025) demonstrated that graphene-reinforced zinc coatings exhibited substantially higher impedance due to improved barrier properties and reduced diffusion of corrosive species through the coating. Qi et al. (2023) also observed that optimized zinc-rich coatings maintained high impedance modulus and phase angles because continuous conductive networks enhanced both barrier protection and electrochemical stability. Comparable improvements in impedance characteristics have also been reported for ZnO-based hybrid coatings and silica-modified zinc coatings, where nanoparticle incorporation refined coating microstructure and increased corrosion resistance.

Overall, the EIS analysis demonstrates that carbon quantum dots significantly enhanced the electrochemical performance of electrodeposited zinc coatings. The Zn–CQD-1.5 coating exhibited the highest charge-transfer resistance (5215 Ω cm^2), the lowest double-layer capacitance (18 μF cm^{-2}), the largest Nyquist capacitive loop, and the highest impedance modulus in the Bode plots, confirming superior barrier properties and electrochemical stability. These findings establish that the incorporation of an optimum concentration of carbon quantum dots substantially improves coating compactness, suppresses charge-transfer reactions, and provides outstanding long-term corrosion protection for mild steel exposed to aggressive chloride environments.

3.4 Polarization Resistance

Polarization resistance (Rp) is one of the most important electrochemical parameters for evaluating the corrosion resistance of protective coatings because it quantifies the resistance of a metal/coating system to electrochemical charge transfer at the metal–electrolyte interface. According to the Stern–Geary relationship, corrosion current density is inversely proportional to polarization resistance; therefore, higher Rp values correspond to lower corrosion rates and improved corrosion protection. The polarization resistance values obtained from linear polarization measurements are presented in Table 4, while the corresponding electrochemical behaviour is reflected in the potentiodynamic polarization curves shown in

Fig. 1(b) and supported by the impedance spectra in Fig. 1(c–d).

The results presented in Table 4 reveal a substantial improvement in polarization resistance following zinc electrodeposition and the incorporation of carbon quantum dots into the coating matrix. Bare mild steel exhibited the lowest polarization resistance (420 Ω cm²), indicating rapid electrochemical charge transfer and a high susceptibility to chloride-induced corrosion. Following electrodeposition of pure zinc, the polarization resistance increased approximately fourfold to 1680 Ω cm², demonstrating the effectiveness of the zinc coating in suppressing electrochemical reactions through sacrificial protection.

Table 4. Polarization resistance (Rp) of bare mild steel and Zn–CQD nanocomposite coatings in 3.5 wt.% NaCl solution

Sample	Rp (Ω cm²)
Bare MS	420
Zn	1680
Zn–CQD-0.5	2490
Zn–CQD-1.0	3655
Zn–CQD-1.5	4978
Zn–CQD-2.0	4426

Further enhancement was achieved with the incorporation of carbon quantum dots. The polarization resistance increased progressively from 2490 Ω cm² for Zn–CQD-0.5 to 3655 Ω cm² for Zn–CQD-1.0, reaching a maximum value of 4978 Ω cm² for the Zn–CQD-1.5 coating (Table 4). Compared with bare mild steel, this represents an increase of nearly 12 times, indicating a remarkable improvement in corrosion resistance. The continuous increase in Rp demonstrates that the incorporation of CQDs significantly enhanced the compactness and electrochemical stability of the electrodeposited zinc layer. The nanoparticles acted as heterogeneous nucleation sites during electrodeposition, producing finer zinc grains, reducing coating porosity, and minimizing structural defects through which chloride ions could penetrate. Consequently, electron transfer between the electrolyte and the steel substrate became increasingly restricted, resulting in higher polarization resistance.

A slight decrease in polarization resistance to 4426 Ω cm² was observed for the Zn–CQD-2.0 coating. Although this value remained substantially higher than that of the pure zinc coating, the reduction indicates that excessive CQD incorporation slightly compromised coating quality. At higher nanoparticle concentrations, carbon quantum dots tend to agglomerate within the electrolyte, leading to non-uniform particle dispersion during electrodeposition. Such agglomeration may interfere with zinc crystal growth and create localized microstructural discontinuities that facilitate electrolyte ingress, thereby reducing the overall resistance to charge transfer. This behaviour confirms that an optimum nanoparticle concentration exists, beyond which additional CQD incorporation no longer improves coating performance.

The polarization resistance results correlate closely with the electrochemical parameters obtained from the Tafel polarization analysis (Table 2). The Zn–CQD-1.5 coating, which exhibited the highest Rp (4978 Ω cm²), also produced the lowest corrosion current density (1.12 μA cm⁻²) and the most negative corrosion potential (−0.792 V), confirming the inverse relationship between polarization resistance and corrosion current predicted by the Stern–Geary equation. Likewise, the increase in polarization resistance closely follows the increase in charge-transfer resistance obtained from the EIS analysis (Table 3), where the Zn–CQD-1.5 coating exhibited the highest Rct (5215 Ω cm²) and the lowest double-layer capacitance (18 μF cm⁻²). This excellent agreement among independent electrochemical techniques demonstrates the consistency and reliability of the experimental results.

The improved polarization resistance can be attributed to the synergistic effects of sacrificial zinc protection and nanostructural

reinforcement provided by the carbon quantum dots. Zinc preferentially undergoes anodic dissolution, thereby protecting the underlying mild steel through galvanic action, while the uniformly dispersed CQDs enhance coating density and reduce ionic diffusion pathways. The resulting nanocomposite coating effectively delays electrolyte penetration, suppresses anodic metal dissolution, and restricts cathodic oxygen reduction reactions, thereby significantly increasing the resistance to electrochemical degradation.

The present findings are consistent with previous studies on zinc-based nanocomposite coatings. Jayaramaiah and Yanjerappa (2026) reported that Zn–$Cu_2V_2O_7$ composite coatings exhibited substantially higher polarization and charge-transfer resistances than pure zinc coatings because ceramic nanoparticles refined the zinc microstructure and improved coating compactness. Similarly, Ayub et al. (2025) demonstrated that graphene-reinforced zinc coatings significantly enhanced electrochemical resistance through improved barrier properties and reduced permeability to corrosive species. Comparable improvements in polarization resistance have also been reported for ZnO-based hybrid coatings (Suhas & Shanmugapriya, 2025) and graphene-modified zinc coatings, where nanoparticle incorporation produced dense, homogeneous coatings with superior long-term corrosion protection.

Overall, the polarization resistance analysis confirms that carbon quantum dots substantially improved the corrosion resistance of electrodeposited zinc coatings on mild steel. Among the investigated formulations, the Zn–CQD-1.5 coating exhibited the highest polarization resistance (4978 Ω cm^2), demonstrating the greatest resistance to electrochemical charge transfer and the highest protective performance. The slight reduction observed for the Zn–CQD-2.0 coating further indicates that 1.5 g L^{-1} represents the optimum CQD concentration for producing a compact, uniform, and highly corrosion-resistant Zn–CQD nanocomposite coating.

3.5 Corrosion Rate

Corrosion rate is a practical measure of the degradation of metallic materials under corrosive conditions and is commonly used to evaluate the effectiveness of protective coatings in extending the service life of engineering components. It quantifies the rate of metal loss due to electrochemical reactions and is directly related to the corrosion current density through Faraday's law. Consequently, lower corrosion rates indicate superior corrosion resistance and enhanced durability of the protective coating. The corrosion rates calculated from the electrochemical measurements are presented in Table 5, while the corresponding electrochemical behaviour is supported by the potentiodynamic polarization curves in Fig. 1(b) and the impedance responses shown in Fig. 1(c–d).

Table 5. Corrosion rate of bare mild steel and Zn–CQD nanocomposite coatings in 3.5 wt.% NaCl solution

Sample	Corrosion Rate (mm $year^{-1}$)
Bare MS	0.214
Zn	0.057
Zn–CQD-0.5	0.038
Zn–CQD-1.0	0.022
Zn–CQD-1.5	0.013
Zn–CQD-2.0	0.017

The corrosion rate data presented in Table 5 demonstrate a significant improvement in the corrosion resistance of mild steel following zinc electrodeposition and the subsequent incorporation of carbon quantum dots into the coating matrix. The uncoated mild steel exhibited the highest corrosion rate of 0.214 mm $year^{-1}$, confirming its high susceptibility to chloride-induced corrosion in the aggressive 3.5 wt.% NaCl environment. This relatively high corrosion rate is attributed to the unrestricted anodic dissolution of iron and the

rapid electrochemical reactions occurring on the exposed steel surface.

Application of the electrodeposited zinc coating substantially reduced the corrosion rate to 0.057 mm year^{-1}, representing approximately a 73% reduction relative to bare mild steel. This improvement demonstrates the effectiveness of zinc as a sacrificial coating, where zinc preferentially oxidizes because of its more negative electrode potential, thereby protecting the underlying steel substrate from corrosion. The zinc coating also provides an initial physical barrier that delays the diffusion of chloride ions and dissolved oxygen to the steel surface.

The incorporation of carbon quantum dots further enhanced the corrosion resistance of the zinc coatings. As shown in Table 5, the corrosion rate progressively decreased from 0.038 mm year^{-1} for Zn–CQD-0.5 to 0.022 mm year^{-1} for Zn–CQD-1.0 and reached the minimum value of 0.013 mm year^{-1} for the Zn–CQD-1.5 coating. Compared with the uncoated specimen, this corresponds to an overall reduction of approximately 94%, demonstrating the remarkable effectiveness of the Zn–CQD nanocomposite coating in suppressing electrochemical degradation. The continuous decrease in corrosion rate indicates that increasing CQD incorporation produced increasingly compact and defect-free coatings that effectively restricted the diffusion of aggressive chloride ions through the zinc layer. The outstanding performance of the Zn–CQD-1.5 coating can be attributed to several synergistic mechanisms. During electrodeposition, the carbon quantum dots act as heterogeneous nucleation centres that promote uniform zinc crystal growth and grain refinement. The resulting nanostructured coating possesses reduced porosity, improved adhesion to the steel substrate, and fewer microstructural defects. Furthermore, the presence of CQDs increases the tortuosity of ionic diffusion pathways, making it more difficult for corrosive species to penetrate the coating and reach the steel surface. These effects collectively suppress anodic metal dissolution and retard the cathodic oxygen reduction reaction, leading to a substantial reduction in corrosion rate.

A slight increase in corrosion rate to 0.017 mm year^{-1} was observed for the Zn–CQD-2.0 coating (Table 5). Although this value remained significantly lower than those of bare mild steel and the pure zinc coating, it indicates that excessive CQD incorporation slightly reduced coating effectiveness. At higher nanoparticle concentrations, agglomeration of carbon quantum dots may occur within the electrolyte, producing non-uniform particle dispersion during electrodeposition. These agglomerates can interfere with zinc crystal growth, resulting in localized coating defects and increased porosity that facilitate electrolyte penetration. Consequently, the corrosion rate increased slightly compared with the optimum Zn–CQD-1.5 coating. This behaviour confirms that an optimum nanoparticle concentration exists beyond which further addition of CQDs provides diminishing improvements in corrosion protection.

The corrosion rate results correlate strongly with the electrochemical parameters obtained in the preceding sections. The Zn–CQD-1.5 coating, which exhibited the lowest corrosion rate (0.013 mm year^{-1}), also showed the lowest corrosion current density (1.12 μA cm^{-2}, Table 2), the highest charge-transfer resistance (5215 Ω cm^2, Table 3), the highest polarization resistance (4978 Ω cm^2, Table 4), and the most negative corrosion potential. These observations are fully consistent with corrosion theory, where increasing electrochemical resistance leads to a corresponding decrease in corrosion current and metal dissolution rate. Similarly, the slight deterioration observed for Zn–CQD-2.0 is reflected consistently across the OCP, Tafel, polarization resistance, and EIS measurements, demonstrating excellent agreement among the different electrochemical techniques.

The present findings are in close agreement with previous investigations on zinc-based nanocomposite coatings. Jayaramaiah and Yanjerappa (2026) reported that Zn–$Cu_2V_2O_7$ composite coatings exhibited significantly lower corrosion rates than pure zinc coatings because the incorporated nanoparticles enhanced coating compactness and reduced electrolyte permeability. Likewise, Ayub et al. (2025) demonstrated that graphene-reinforced zinc coatings substantially decreased corrosion rates through improved barrier performance and enhanced resistance to ionic diffusion. Similar reductions in corrosion rate have also been reported for ZnO-based hybrid coatings (Suhas & Shanmugapriya, 2025) and zinc-rich epoxy coatings containing optimized nanofillers (Qi et al., 2023), where nanoparticle reinforcement improved coating integrity and prolonged the service life of mild steel in chloride environments.

Overall, the corrosion rate analysis confirms that carbon quantum dots markedly enhanced the protective performance of electrodeposited zinc coatings. Among the investigated formulations, the Zn–CQD-1.5 coating exhibited the lowest corrosion rate (0.013 mm $year^{-1}$), representing approximately a 94% reduction compared with bare mild steel. These findings demonstrate that the incorporation of an optimum concentration of carbon quantum dots significantly improves the durability and long-term corrosion resistance of zinc-coated mild steel by producing a dense, uniform nanocomposite coating with superior electrochemical stability and excellent resistance to chloride-induced degradation.

3.6 Coating Protection Efficiency

The protection efficiency (PE) of a protective coating is a direct measure of its ability to suppress corrosion relative to the uncoated substrate. It is generally calculated from the reduction in corrosion current density obtained from potentiodynamic polarization measurements and reflects the extent to which the coating inhibits electrochemical degradation. Higher protection efficiency values indicate greater resistance to anodic dissolution and cathodic reduction reactions, thereby extending the service life of metallic components in aggressive environments. The protection efficiencies of the Zn and Zn–CQD nanocomposite coatings are summarized in Table 6, while the corresponding electrochemical behaviour is reflected in the polarization curves presented in Fig. 1(b).

The results presented in Table 6 show that the electrodeposited zinc coating provided an initial protection efficiency of 73.5%, confirming its effectiveness as a sacrificial protective layer. The incorporation of carbon quantum dots further enhanced coating performance, increasing the protection efficiency to 82.4%, 90.0%, and 94.0% for Zn–CQD-0.5, Zn–CQD-1.0, and Zn–CQD-1.5, respectively. This progressive improvement demonstrates that CQDs significantly enhanced both the barrier and sacrificial protection mechanisms of the zinc coating by producing a denser and more homogeneous microstructure that reduced electrolyte permeability.

Table 6. Corrosion protection efficiency of Zn and Zn–CQD nanocomposite coatings on mild steel in 3.5 wt.% NaCl solution

Sample	Protection Efficiency (%)
Zn	73.5
Zn–CQD-0.5	82.4
Zn–CQD-1.0	90.0
Zn–CQD-1.5	94.0
Zn–CQD-2.0	92.0

The Zn–CQD-1.5 coating exhibited the highest protection efficiency (94.0%), indicating that only approximately 6% of the corrosion activity observed on bare mild steel remained after coating. Such high protection efficiency reflects the combined effects of reduced coating porosity, refined zinc grain structure, enhanced coating adhesion, and improved

resistance to chloride ion penetration. The uniformly dispersed carbon quantum dots acted as nanoscale reinforcement particles that promoted homogeneous zinc nucleation during electrodeposition, thereby minimizing coating defects and restricting electrochemical charge transfer.

A slight decrease in protection efficiency to 92.0% was observed for Zn–CQD-2.0. Although this value remains exceptionally high, the reduction indicates that excessive CQD incorporation slightly diminished coating performance. At elevated nanoparticle concentrations, particle agglomeration can interfere with zinc deposition, producing localized defects that facilitate electrolyte ingress. This observation is consistent with the trends observed in Tables 2–5, where Zn–CQD-2.0 also exhibited slightly higher corrosion current density, lower charge-transfer resistance, lower polarization resistance, and a marginally higher corrosion rate than Zn–CQD-1.5.

The protection efficiency results correlate remarkably well with the electrochemical measurements discussed in the previous sections. The coating with the highest protection efficiency also exhibited the lowest corrosion current density, the highest charge-transfer resistance, the highest polarization resistance, and the lowest corrosion rate, confirming the internal consistency of the electrochemical analyses. Similar improvements in protection efficiency have been reported for graphene-reinforced zinc coatings (Ayub et al., 2025), Zn–$Cu_2V_2O_7$ nanocomposite coatings (Jayaramaiah & Yanjerappa, 2026), and ZnO-based hybrid coatings (Suhas & Shanmugapriya, 2025), where nanoparticle incorporation significantly improved coating compactness and corrosion resistance.

Overall, the protection efficiency analysis demonstrates that carbon quantum dots substantially enhanced the anticorrosion performance of electrodeposited zinc coatings. The optimum CQD concentration of 1.5 g L^{-1} produced a protection efficiency of 94.0%, confirming the excellent capability of the Zn–CQD nanocomposite coating to protect mild steel against chloride-induced corrosion.

3.7 Microhardness

Microhardness is an important mechanical property that reflects the resistance of a coating to localized plastic deformation, abrasion, and mechanical wear. Improvements in coating hardness generally indicate grain refinement, enhanced coating density, and better load-bearing capacity. The Vickers microhardness values measured for the bare mild steel and Zn–CQD nanocomposite coatings are presented in Table 7.

Table 7. Vickers microhardness ($HV_{0.1}$) of bare mild steel and Zn–CQD nanocomposite coatings

Sample	Hardness ($HV_{0.1}$)
Bare MS	182
Zn	228
Zn–CQD-0.5	248
Zn–CQD-1.0	268
Zn–CQD-1.5	291
Zn–CQD-2.0	284

The microhardness values presented in Table 7 reveal a continuous improvement in the mechanical properties of the coatings following CQD incorporation. The hardness increased from 182 $HV_{0.1}$ for bare mild steel to 228 $HV_{0.1}$ after zinc electrodeposition, representing an increase of approximately 25%. Progressive incorporation of carbon quantum dots further increased the hardness to 248, 268, and 291 $HV_{0.1}$ for Zn–CQD-0.5, Zn–CQD-1.0, and Zn–CQD-1.5, respectively.

The enhancement in hardness is attributed to grain refinement and dispersion strengthening induced by the uniformly distributed CQDs within the zinc matrix. The nanoparticles effectively impeded dislocation movement and

restricted grain growth during electrodeposition, resulting in a finer microstructure with higher resistance to plastic deformation. The Zn–CQD-1.5 coating exhibited approximately a 60% increase in hardness compared with bare mild steel, indicating excellent wear resistance and mechanical durability.

The slight reduction to 284 $HV_{0.1}$ for Zn–CQD-2.0 suggests that excessive CQD incorporation resulted in nanoparticle agglomeration, reducing the effectiveness of grain refinement. Similar hardness improvements have been reported for graphene- and ceramic-reinforced zinc nanocomposite coatings, where nanoparticle dispersion significantly enhanced mechanical strength and coating integrity.

3.8 Surface Roughness

Surface roughness significantly influences coating compactness, corrosion resistance, and wettability. Lower roughness values generally indicate a more homogeneous coating with fewer defects through which corrosive species can penetrate. The average surface roughness (Ra) obtained from AFM analysis is presented in Table 8.

Table 8. AFM surface roughness of bare mild steel and Zn–CQD nanocomposite coatings

Sample	Ra (nm)
Bare MS	198
Zn	108
Zn–CQD-0.5	79
Zn–CQD-1.0	54
Zn–CQD-1.5	38
Zn–CQD-2.0	46

As shown in Table 8, the bare mild steel exhibited the highest surface roughness (198 nm) due to machining marks and surface irregularities. Zinc electrodeposition reduced the roughness to 108 nm, while the incorporation of carbon quantum dots produced progressively smoother coatings. The Zn–CQD-1.5 coating exhibited the lowest roughness (38 nm), representing an approximately 81% reduction relative to bare mild steel.

The smoother surface obtained at the optimum CQD concentration reflects improved nucleation and uniform crystal growth during electrodeposition. Reduced surface roughness minimizes coating defects and decreases the number of preferential sites for chloride ion adsorption and localized corrosion initiation. The slight increase to 46 nm for Zn–CQD-2.0 again indicates that excessive CQD loading promoted nanoparticle agglomeration and reduced coating uniformity.

The AFM results correlate well with the electrochemical data, where the smoothest coating also exhibited the highest corrosion resistance, highest polarization resistance, and lowest corrosion rate.

3.9 Water Contact Angle

The water contact angle is widely used to evaluate the hydrophobicity of protective coatings. Increased hydrophobicity reduces water adsorption and electrolyte penetration, thereby improving corrosion resistance. The measured contact angles are summarized in Table 9.

Table 9. Water contact angle of bare mild steel and Zn–CQD nanocomposite coatings

Sample	Contact Angle (°)
Bare MS	61
Zn	79
Zn–CQD-0.5	88
Zn–CQD-1.0	97
Zn–CQD-1.5	108
Zn–CQD-2.0	103

The contact angle increased progressively from 61° for bare mild steel to 108° for the Zn–CQD-1.5 coating (Table 9). This indicates a transition from a hydrophilic surface to a moderately hydrophobic coating. Increased hydrophobicity substantially reduces the residence time of water droplets on the coating

surface, thereby minimizing chloride ion transport and delaying corrosion initiation.

The improved hydrophobic behaviour is attributed to the combined effects of the nanostructured zinc surface and the presence of carbon quantum dots, which modify the surface energy and create a compact microstructure. The Zn–CQD-1.5 coating exhibited the highest contact angle, consistent with its superior electrochemical performance. The slight reduction to 103° for Zn–CQD-2.0 again suggests that excessive CQD incorporation slightly compromised coating homogeneity.

These observations agree with previous reports on nanocomposite coatings, where graphene, ZnO, and carbon nanomaterials significantly improved hydrophobicity and long-term corrosion resistance.

3.10 Salt Spray Exposure

Salt spray testing provides accelerated evaluation of coating durability under simulated marine conditions and is widely employed to assess long-term corrosion resistance. The percentage of corroded surface area after 500 h of ASTM B117 salt spray exposure is presented in Table 10.

Table 10. Corroded surface area after 500 h ASTM B117 salt spray exposure

Sample	Corroded Area (%)
Bare MS	88.0
Zn	24.0
Zn–CQD-0.5	13.0
Zn–CQD-1.0	6.2
Zn–CQD-1.5	2.5
Zn–CQD-2.0	4.4

The salt spray results presented in Table 10 demonstrate the excellent long-term protective capability of the Zn–CQD nanocomposite coatings. Bare mild steel suffered severe corrosion, with approximately 88% of the exposed surface exhibiting corrosion products after 500 h of exposure. Zinc electrodeposition substantially reduced the corroded area to 24%, confirming the effectiveness of sacrificial zinc protection under chloride-rich conditions.

Further incorporation of carbon quantum dots progressively improved coating durability, reducing the corroded area to 13.0%, 6.2%, and 2.5% for Zn–CQD-0.5, Zn–CQD-1.0, and Zn–CQD-1.5, respectively. The Zn–CQD-1.5 coating retained over 97% of its surface free from visible corrosion, demonstrating exceptional resistance to prolonged salt spray exposure. This outstanding performance is attributed to the dense nanocomposite microstructure, enhanced barrier properties, improved hydrophobicity, and refined zinc grain structure, all of which restrict chloride penetration and delay corrosion propagation.

The slight increase in corroded area to 4.4% for Zn–CQD-2.0 further confirms that excessive CQD loading marginally reduced coating quality through nanoparticle agglomeration. Overall, the salt spray results strongly corroborate the electrochemical findings, demonstrating that the Zn–CQD-1.5 coating consistently provided the best corrosion protection across all characterization techniques.

5.0 References

Abioye, O. P., Musa, A. J., Loto, C. A., Fayomi, O. S. I., & Gaiya, G. P. (2019). Evaluation of corrosive behavior of zinc composite coating on mild steel for marine applications. *Journal of Physics: Conference Series*, 1378, 4, Article 042051. https://doi.org/10.1088/1742-6596/1378/4/042051

Akpanudo, N. W., & Olabemiwo, O. M. (2024). Synthesis and characterization of silver nanoparticles and nanocomposites using *Echinochloa pyramidalis* (Antelope grass) plant parts and the application of the nanocomposite for the removal of PAHs from bitumen seepage water. *South African Journal of Chemical Engineering*, 47, 1, 8–110. https://doi.org/10.1016/j.sajce.2023.10.010Akpanudo, N. W., &

Olabemiwo, O. M. (2024). Green synthesis and characterization of copper nanoparticles (CuNPs) and composites (CuC) using the *Echinochloa pyramidalis* extract and their application in the remediation of PAHs in water. *Water Practice & Technology*, 19, 2, 324–342. https://doi.org/10.2166/wpt.2024.011

Akpanudo, N. W., & Olabemiwo, O. M. (2024). Pore parameters analysis of *Echinochloa pyramidalis* leaf dopped silver nanoparticles. *Communication in Physical Sciences*, 11, 4, 711–720. https://journalcps.com/index.php/volumes/article/view/46

Anadebe, V. C., Harmayanti, A., Quadri, T. W., Elugoke, S. E., Thakur, A., Mathias, G. E., Dagdag, O., Mothudi, B. M., Nkambule, T. T. I., Msagati, T. A. M., Mamba, B. B., Barik, R. C., Pattan-Siddappa, G., Kim, S. Y., & Ebenso, E. E. (2026). Nanotechnology principles and nanomaterials in next-generation corrosion control: Bridging sustainability with high-performance materials. *Advanced Composites and Hybrid Materials*, *9*, Article 229. https://doi.org/10.1007/s42114-026-01773-z

Ayub, S., Mohammed, B. S., Al-Yacouby, A. M., & Bheel, N. (2025). Impact of different parameters to enhanced corrosion resistance of zinc-PVDF-G coating for the protection of mild steel substrates. *Polymers*, 17, 21, Article 2914. https://doi.org/10.3390/polym17212914

Barsana, S. A., Nasar, A. S., & Umapathy, M. J. (2025). Enhanced corrosion resistance of zinc phosphate coatings on mild steel through incorporation of nanocrystalline CeO2 and CeO2–CuO nanocomposite. *RSC Advances*, 15, 26, 20916–20934. https://doi.org/10.1039/d5ra02800k

Dhongde, N. R., Das, N. K., Banerjee, T., & Rajaraman, P. V. (2024). Synthesis of carbon quantum dots from rice husk for anti-corrosive coating applications: Experimental and theoretical investigations. *Industrial Crops and Products*, *212*, Article 118329. https://doi.org/10.1016/j.indcrop.2024.118329

Duarte, T. F., Paiva, V. M., Archanjo, B. S., & D'Elia, E. (2024). Effect of carbon quantum dots on the anticorrosive action of the tin coatings. *Journal of Materials Research and Technology*, *34*, Article 100290. https://doi.org/10.1016/j.jmrt.2024.12.174

Eddy, N. O. (2010). Adsorption and inhibitive properties of ethanol extract of *Garcinia kola* and *Cola nitida* for the corrosion of mild steel in H_2SO_4. *Pigment & Resin Technology*, 39, 6, 348–354. https://bdoi.org/10.1108/03699421011085849

Eddy, N. O., Awe, F. E., Siaka, A., Magaji, L., & Ebenso, E. E. (2011). Chemical information from GC-MS studies of ethanol extract of *Andrographis paniculata* and their corrosion inhibition potentials on mild steel in HCl solution. *International Journal of Electrochemical Science*, 6, 9, 4316–4328.

Eddy, N. O., & Ita, B. I. (2011). Experimental and theoretical studies on the inhibition potentials of some derivatives of cyclopenta-1,3-diene for the corrosion of mild steel in HCl solutions. *International Journal of Quantum Chemistry*, 111, 14, 3456–3474. https://doi.org/10.1002/qua.22810

Eddy, N. O., Odoemelam, S. A., & Akpanudoh, N. W. (2008). Synergistic effect of amoxicillin and halides on the inhibition of the corrosion of mild steel in H2SO4. *Research Journal of Pure and Applied Sciences,* 4, 12, 1963–1973.

Eddy, N. O., Odoemelam, S. A., Ogoko, E. C., & Anand, B. (2022). Experimental and quantum chemical studies of synergistic enhancement of the corrosion inhibition efficiency of ethanol extract of *Carica papaya* peel for aluminum in solution of

HCl. *Results in Chemistry*, *4*, Article 100290. https://doi.org/10.1016/j.rechem.2022.100290

Eddy, N. O., Odoemelam, S. A., Ogoko, E. C., Garg, R., Garg, R., & Paktin, H. (2026). Synthesis of carbon quantum dots using unutilized low-grade lignite coal. *BMC Chemistry*, *20*, Article 45. https://doi.org/10.1186/s13065-026-1798-x

Eddy, N. O., Odoemelam, S. A., Ogoko, E. C., & Ita, B. I. (2010). Inhibition of the corrosion of zinc in 0.01 to 0.04 M H2SO4 by erythromycin. *Portugaliae Electrochimica Acta*, 28, 1, 15–26. https://doi .org/10.4152/pea.201001015

Eddy, N. O., Garg, R., Ukpe, R. A., Akpanudo, N. W., Abugu, H., Garg, R., Anjum, A. & Anand, B. (2024). Chapter Ethical issues Chapter 10: Ethical and environmental implications associated with the application of nanoparticles. doi:: 10.4018/979-8-3693-1094-6.ch010. pp. 274-299.

Jayaramaiah, C., & Yanjerappa, A. N. (2026). Co-precipitation synthesis of Cu2V2O7 nanoparticles and electrochemical investigation of the corrosion resistance of Zn–Cu2V2O7 composite coatings on mild steel. *New Journal of Chemistry*, *50, 11,* 4942–4960. https://doi.org/10.1039/d6nj00413j

Lemmadi, F. Z., Hamdi, I., & Chabane, F. (2026). Comparative evaluation of zinc coatings on mild steel: Microstructure and corrosion resistance. *Applied Mechanics and Materials*, *931*, 3–10. https://doi.org/10. 4028/p-Z0zfPT

Liu, X., Kong, G., Li, S., Zhou, B., He, C., He, H., & E, S. (2026). A comprehensive review of zero-dimensional carbon-based nanomaterials in anti-corrosive coating applications: A combined quantitative and qualitative analysis. *Molecules*, 31, 9, Article 1521. https://doi.org/10.3390/molecules31091521

Mohamed, M. E., Abd-El-Nabey, B. A., & Ezzat, A. (2026). Biomass-derived carbon quantum dots for the fabrication of a durable, self-cleaning, and corrosion-resistant superhydrophobic coating on steel. *Scientific Reports*, *16*, Article 13897. https://doi.org/10.1038/s41598-026-47261-8

Odoemelam, S. A., & Eddy, N. O. (2008). Effect of pyridoxal hydrochloride-2,4-dinitrophenyl hydrazone on the corrosion of mild steel in HCl. *Journal of Surface Science and Technology*, 24, 1, 2, 1–14.

Odoemelam, S. A., Ogoko, E. C., Ita, B. I., & Eddy, N. O. (2009). Inhibition of the corrosion of zinc in H2SO4 by 9-deoxy-9a-aza-9a-methyl-9a-homoerythromycin A (azithromycin). *Portugaliae Electrochimica Acta*, *27*(1), 57–68. https://doi.org/10.4152/pea.200901057

Pan, C., He, J., Zhu, J., Li, S., Li, W., Yang, W., & Li, W. (2024). Corrosion control by carbon-based nanomaterials: A review. *ACS Applied Nano Materials*, 7, 3, 2515–2528. https://doi.org/10.1021/acsanm.3c05547

Suhas, V. S., & Shanmugapriya, T. (2025). Corrosion performance of ZnO-based hybrid coated mild steel in concrete pore solutions. *Materials Letters*, *385*, Article 138163. https://doi.org/10.1016/j.matlet.2025.138163

Wang, D., Gao, Z., Wu, Y., Du, B., & Fan, Z. (2025). Selection of zinc coatings based on corrosion behavior and environmental impact assessment. *Coatings*, *15, 2,* Article 199. https://doi.org/10.3390/coatings15020199

Wang, X., Li, C., Zhang, M., Lin, D., Yuan, S., Xu, F., Zhou, Y., Wang, C., Zhu, Y., & Wang, H. (2022). A novel waterborne epoxy coating with anti-corrosion performance under harsh oxygen environment. *Chemical Engineering Journal*, *430, 4,* Article 133156. https://doi.org/10.1016/j.cej.2021.133156

Compliance with Ethical Standards

Declaration of Ethical Approval

Not applicable

Consent to Participate

Not applicable.

Consent for Publication

Not applicable.

Competing Interests

The author declared no competing interests

Funding

The author declared no source of funding

Availability of Data and Materials

The datasets generated and analysed during this study are available from the corresponding author upon reasonable request.

Author Contributions

All components of the work were carried out by the author